2024

Modeling and Experimental Validation of the Thermophysical Properties of a POE+R1233zd(E) Mixture

Nicolas Leclercq
n.leclercq@uliege.be

Katharina Stöckel
katharina.stoeckel@tu-dresden.de

Christiane Thomas
christiane.thomas@tu-dresden.de

Vincent Lemort
vincent.lemort@uliege.be

Modeling and experimental validation of the thermophysical properties of a POE+R1233zd(E) mixture

Nicolas LECLERCQ[1*], Katharina STOECKEL[2], Christiane THOMAS[2], Vincent LEMORT[1]

[1] University of Liège, Thermodynamics Laboratory,
Liège, Belgium

[2] Technische Universität Dresden, Schaufler Chair of Refrigeration, Cryogenics and Compressor Technology,
Dresden, Germany

*Corresponding Author (n.leclercq@ULiege.be)

ABSTRACT

Reliable data of the properties of lubricant + refrigerant mixtures are essential in many applications to assess the behavior of refrigeration and heat pump systems. The accurate modeling of all required thermophysical properties (including density, viscosity, thermal conductivity, enthalpy, entropy, and phase equilibria) remains a key challenge today.

In this work, thermophysical property measurements of a "pure" POE lubricant and its mixture with the refrigerant R1233zd(E) were carried out in the temperature range from 283.15 to 373.15 K with pressures up to 1.2 MPa, using experimental facitilies from the Technische Universität Dresden. Based on the modelling approach developed by Yang et al. (Ind. Eng. Chem. Res. 2023, 44, 18736–18749), the thermophysical properties of the "pure" POE and its mixture with R1233zd(E) are modeled in much larger temperature and pressure ranges. This model is a semi-empirical approach making use of a small amount of experimental data (density, viscosity, thermal conductivity and heat capacity) of the pure lubricant to obtain the lubricant's fluid constants (e.g., critical temperature). Subsequently, some experimental bubble point pressure data of the mixture were used to fit the binary interaction parameters in mixing rules, which enable mixture predictions. The predictions of this model are compared with those of the classical empirical models employed for lubricant + refrigerant mixtures, specifically the Henderson equations for density and viscosity, and the Cavestri equation for the vapor pressure. The results show a better agreement with the experimental data for the empirical modeling approach for both the density and viscosity, while the vapor pressure data prediction accuracies are even for both approaches. In particular, the viscosity prediction of the thermodynamic approach are not good for the mixture, with a root mean square relative error of 40%. Finally, the two modelling approaches are compared on other modeling aspects than accuracy, for instance, the number of experimental data required, the ability to predict other properties and the physical sense of the calibrated parameters, making the approach developed by Yang et al. a convenient option in many applications.

1. INTRODUCTION

In vapor compression refrigeration and heat pump systems with positive displacement compressors, oil is necessary to ensure a good lubrication of the compressor. The presence of this oil is required to avoid premature wear between moving parts by creating a thin film avoiding direct contact between metallic surfaces. Moreover, the oil can act as a sealant in the leakage gaps and allows to reduce the discharge temperature thereby minimizing mechanical stress induced by large temperature differences (Bell, 2011). Nevertheless, the presence of oil in thermodynamic cycle also presents some drawbacks (Youbi-Idrissi and Bonjour, 2008). First of all, it reduces the heat transfer coefficient in the heat exchangers, especially in the two-phase region, implying the use of bigger heat exchangers. Moreover, it reduces the cooling capacity of refrigeration cycles by not allowing a full evaporation of the refrigerant as a part of this refrigerant that is solved in the oil stays in the liquid phase. More pressure losses are also faced in micro-channel heat exchangers due to the high oil viscosity. Finally, it modifies the thermodynamic properties of the refrigerant (enthalpies, densities, vapor-liquid equilibria, etc.), making the evaluation of cycle performance more difficult, especially when high oil fractions are used.

The Horizon 2020 EU-funded project REGEN-BY-2 consists of the development of a trigeneration machine allowing the simultaneous generation of electric, thermal and/or cooling powers in one single system by making use of two-

phase refrigerant compressions/expansions (Briola et al., 2021). In the frame of this project, the necessity for high oil circulation ratios in the two-phase scroll machines is of paramount importance in order to guarantee the required lubrication. To counterbalance the reduction of viscosity due to the presence of refrigerant in the liquid phase, high oil fractions (up to 20%) are used. Furthermore, this high oil fraction combined with low vapor qualities of the two-phase mixture implies difficulties in the calculations of the compressor performance, more specifically in the inlet/outlet enthalpy/entropy calculations. In Leclercq et al. (2024), the authors investigate the behavior of an off-the-shelf scroll compressor under two-phase oil-refrigerant flows. The definition of the volumetric and isentropic efficiencies of this two-phase oil-refrigerant mixture compression are detailed, they require the definition of two-phase mixture density, entropy and enthalpy, calculated as a combination of oil, saturated liquid and superheated vapor properties. When high oil circulation ratios are also investigated, but with high superheats, the solubility of the refrigerant in the oil can be neglected, however, the property of the oil still needs to be taken into account in the mixture property (Ramaraj et al., 2014). Finally, when low oil fractions are used (< 5% in mass), its effect is usually totally neglected and the resulting mixture properties are simply the properties of the pure refrigerant.

For the sake of improvement of the post-processing analysis proposed in Leclercq et al. (2024), the oil-refrigerant mixture properties will be experimentally investigated and some models proposed to fit the collected data. The refrigerant used is the HCFO-R1233zd(E) and it is combined with a lubricant, the POE Emkarate RL32 MAF. The mixture properties investigated in this paper includes the liquid-vapor equilibrium (vapor pressure, or more specifically, bubble point pressure), the density and the dynamic viscosity. In the first section, the experimental measurements performed on the oil-refrigerant mixture will be detailed. The measurement setups will be presented along with the uncertainties of the sensors used to measure the required properties. In the second section, several techniques used to model mixture properties will be presented. In the third section, the models presented in section two are going to be validated and the results accuracy are compared.

2. EXPERIMENTAL MEASUREMENTS

The experimental data used for this work have been collected using experimental setups from the Schaufler Chair of Refrigeration, Cryogenics and Compressor Technology of the Technische Universität Dresden. Two setups have been used: one for conducting vapor-liquid equilibrium measurements, and another for determining density and viscosity of the mixture in the liquid phase.

2.1 Liquid-vapor equilibrium

The liquid-vapor equilibrium experimental setup consists of some hand-made iso-volume units using glass tubes. The glass allows to measure the liquid height, and thus to deduce the volume taken by the vapor and also to detect potential miscibility gaps. The objective is, for several oil-refrigerant liquid compositions, to measure the bubble points pressures as a function of the temperature. Information regarding this setup have already been published; more details can be found in Stöckel et al. (2023). Four tubes filled with the mixture (known composition) are placed inside a climate chamber allowing temperature regulation, as shown in Figure 1. Each tube is composed of a valve allowing the filling, and of two sensors to get the temperature and the pressure, as can be seen in Figure 2. The tubes need to be shaken every 5 minutes to reach a stable pressure equilibrium, using a shaft connecting them together and providing an access outside the chamber. Two to three hours are required to get 4 measurements points (from the four tubes) for a single temperature. The volumes of each four units are initially measured using pressurized nitrogen (the length of the pipe can vary from one another), however, the mass of the injected nitrogen being very low, a lot of uncertainty is faced as can be seen in Figure 3. Nevertheless, as this uncertainty only impacts the volume taken by the vapor phase (the liquid volume being directly measured through the glass), which has a negligible mass in comparison to the liquid, it does not impact consequently the final refrigerant liquid fraction determined. The used sensors of the two experimental setups along with their ranges and uncertainties are presented in Table 1.

2.2 Density and viscosity

The density-viscosity setup consists in a cycle placed inside a climate chamber using a pump to circulate the mixture. The cycle diagram can be found in Figure 4. The objective of this setup is to measure the liquid phase mixture properties (speed of sound, density, viscosity) for different temperatures set by the climate chamber. To vary the composition of the mixture, some oil or refrigerant can be added inside the cycle, until the maximum volume is reached. To obtain low refrigerant fractions, the setup was first filled with oil, and refrigerant was added little by little with a known mass in order to know the refrigerant fraction. On the contrary, for high refrigerant fractions, the refrigerant is added first,

and the oil is added little by little, until reaching the maximum volume of the unit.

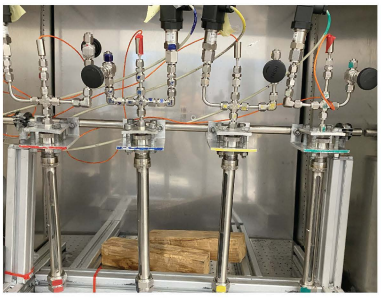

Figure 1: Tubes inside the climate chamber.

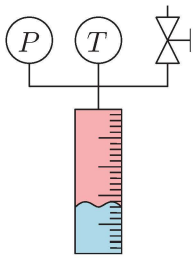

Figure 2: Representation of an iso-volume unit.

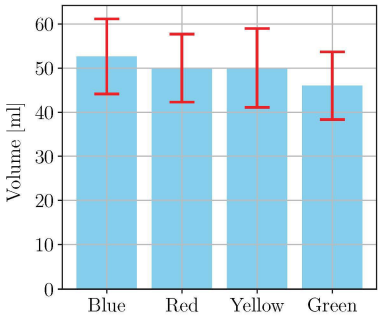

Figure 3: Volumes of the four units with uncertainties

Table 1: Sensors used, range and uncertainties.

Sensor	Equipment	Range	Uncertainty
Scale	Kern PFB	0 - 3000 [g]	0.05 [g]
Temperature LV	PT100	-75 - 250 [°C]	0.5 [K]
Pressure LV	Keller PA-21y	0 - 25 [bara]	0.125 [bar]
Viscometer 1	Cambridge ViscoPRO 2100 - Piston	2.5 - 50 [mPa·s]	0.5 [mPa·s]
Viscometer 2	Cambridge ViscoPRO 2100 - Volumetric flask	0.25 - 5 [mPa·s]	0.05 [mPa·s]
Densimeter	Anton Paar L-DENS 7400	0 - 3000 [kg/m^3]	0.1 [kg/m^3]

1. Gear pump
2. Cambridge viscometers
3. Anton Paar densimeter
4. Anton Paar sound velocity meter
5. Pressure tank
6. 70 bar overpressure valve
7. Sight glass
8. Needle valve
9. High pressure plug valve
10. Plug valve
11. Keller 50 bar pressure sensor
12. Temperature sensor Pt100
13. Climate chamber

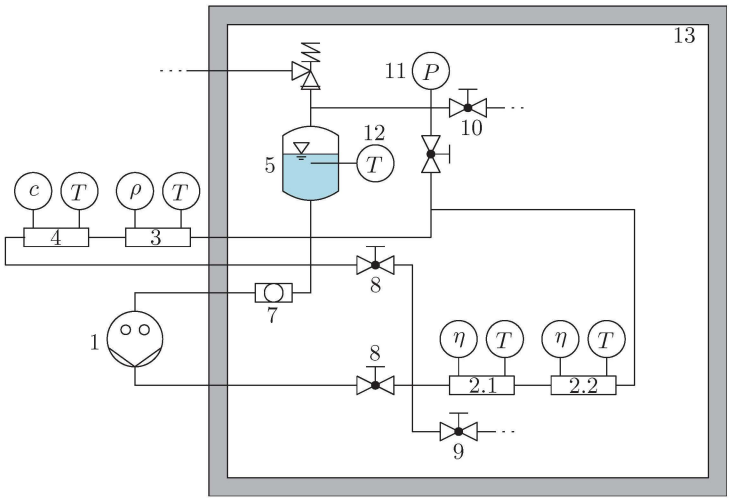

Figure 4: Diagram of the viscosity-density measurement setup

The sensors used in this setup along with their ranges and uncertainties can be found in Table 1. The speed of sound meter details are not given here as this property is not investigated in the paper, the data is however available and can be requested from the authors.

3. MODELING OF OIL-REFRIGERANT MIXTURES

3.1 Liquid-vapor equilibrium

When oil is added to a refrigerant, its liquid-vapor equilibrium is changed. In fact, the more oil is added to a refrigerant, the more refrigerant is solved in the oil (in the liquid phase), resulting in a zeotropic behavior of the mixture. One can

therefore differentiate the temperature/pressure of the bubble point, where the evaporation of the mixture starts and vapor quality increases, by increasing the temperature or decreasing the pressure, and of the dew point, where a full evaporation can be achieved. In oil-refrigerant mixtures, however, the dew point is usually not reachable, as the high temperature required would imply oil degradation. In fact, the saturation pressure at room temperature of an oil is extremely low (Scialdone et al., 1996), which explains the need for very high temperature to vaporize this oil. The solubility curves, showing the refrigerant composition in the liquid phase can be represented in diverse ways. In this paper, P-x-T diagrams are going to be employed. The vapor pressure (or bubble points pressures) will therefore be determined as a function of the refrigerant liquid mass fraction and the temperature.

Vapor pressure predictive models can be classified in two categories: empirical and thermodynamic approaches. Among the empirical approaches, lots of correlations can be found. For instance, a model with one single empirical parameter, based on Raoult's law, is proposed by Dawo et al. (2021). In this paper, the focus will be placed on the Cavestri equation (Cavestri, 1995). This equation constitutes a modified Raoult's law, where 6 empirical parameters (a_1 to a_6) need to be fitted. Such equation usually requires a lot of data to be accurate over a wide range of temperatures and refrigerant liquid fractions. The Cavestri equation can be found in Equation 1, where P^{σ}_{ref} stands for the saturation pressure of the pure refrigerant at a given temperature. It is important to note that the refrigerant liquid fraction x_{ref} is a molar fraction expressed here in [refrigerant liquid mol/liquid mol].

$$P(x_{\text{ref}}, T) = x_{\text{ref}} P^{\sigma}_{\text{ref}}(T) + x_{\text{ref}} \cdot (1 - x_{\text{ref}}) \cdot (a_1 + a_2 T + a_3 T^2 + a_4 + a_5 x_{\text{ref}} T + a_6 x_{\text{ref}} T^2) \tag{1}$$

Regarding thermodynamic models, several modeling techniques exist to determine the liquid-vapor equilibrium. They are all based on the phases fugacities equality, which translates as a state where Gibbs free energy is minimum. The vapor pressure can, for instance, be computed using a mixing rule applied to an equation of state (EoS) to figure out the fugacities of the two phases as done by Neto and Barbosa (2011), or using an activity coefficient model to compute the liquid phase fugacity and assuming an ideal gas fugacity as proposed by Jia et al. (2020). Thermodynamic models usually require a few number of experimental data to be validated.

In this paper, a thermodynamic model is going to be employed and its results will be compared with the results of the Cavestri equation mentioned earlier. The approach is based on the methodology proposed by Yang et al. (2023a), where the thermophysical properties of lubricants, considered as "pure entities" and their mixtures with refrigerants are modeled. This model makes use of a small amount of experimental data (density, viscosity, thermal conductivity and heat capacity) of the "pure" lubricant to obtain the fluid constants (e.g., critical temperature) required in the Patel-Teja-Valderrama (PVT) cubic equation of state (Patel and Teja, 1982) (Valderrama, 1990) and residual entropy scaling approaches (Yang et al., 2022) (Yang et al., 2023b). This approach is therefore allowing not only to get liquid-vapor equilibrium points, but to get a complete set of thermophysical properties and transport properties, and will therefore be used to predict the density and the viscosity as well.

3.2 Density and viscosity

The density and the viscosity of an oil-refrigerant mixture liquid phase can also be predicted by using empirical correlations. However, no empirical correlation can predict accurately the density/viscosity for both high and low refrigerant mass fractions. Henderson (1994) proposes two correlations for both viscosity and density, for low (< 30%) and high (> 70%) refrigerant mass fractions and each of them uses 9 empirical parameters (from a_1 to a_9). These correlations are going to be calibrated in this paper. For low refrigerant mass fractions, the two equations (respectively for the density and the viscosity) can be written as follows:

$$\rho(w_{\text{ref}}, T) = [a_1 + a_2 T + a_3 T^2] + w_{\text{ref}}[a_4 + a_5 T + a_6 T^2] + w^2_{\text{ref}}[a_7 + a_8 T + a_9 T^2] \tag{2}$$

$$\log(\log(\eta(w_{\text{ref}}, T) + 0.7)) = [a_1 + a_2 \log(T) + a_3 \log^2(T)] + w_{\text{ref}}[a_4 + a_5 \log(T) + a_6 \log^2(T)] + w^2_{\text{ref}}[a_7 + a_8 \log(T) + a_9 \log^2(T)] \tag{3}$$

For high refrigerant mass fractions, the equations are:

$$\rho(w_{\text{ref}}, T) = [a_1 + a_2 T_r + a_3 T_r^2] + w_{\text{ref}}[a_4 + a_5 T_r + a_6 T_r^2] + w^2_{\text{ref}}[a_7 + a_8 T_r + a_9 T_r^2] \tag{4}$$

$$\log(\eta(w_{\text{ref}}, T)) = [a_1 + a_2/T + a_3/T^2] + w_{\text{ref}}[a_4 + a_5/T + a_6/T^2] + w^2_{\text{ref}}[a_7 + a_8/T + a_9/T^2] \tag{5}$$

Where T_r is a reduced temperature defined as $T_r = 1 - T/T_c$. The logarithm used (log) is of base 10. In all above equations, w_{ref} is a mass fraction expressed in [liquid refrigerant kg/liquid kg].

The approach developed in Yang et al. (2023a) can also be applied to determine the density and the viscosity of the mixture liquid phase and this prediction will be detailed later in this paper. The density is simply an output of the PVT equation of state of the mixture for a given pressure and temperature as will be detailed in the subsequent section. The viscosity can be predicted using a residual entropy scaling technique, where 3 or 4 parameters need to be fitted. This modeling technique creates a link between the residual entropy, deviation in entropy from the real gas and the ideal gas, and the residual viscosity. More details can be found in Yang et al. (2022).

4. MODELS VALIDATION

4.1 Approach of Yang et al. (2023a) (Thermodynamic model)

In the modeling approach proposed by Yang et al. (2023a), the lubricant (i.e., POE Emkarate RL32 MAF) must be characterized as a pure fluid using the PVT equation of state and a residual entropy scaling approach for the viscosity. Thereby, the following steps must be carried out, and this procedure has been implemented in the software package OilMixProp 1.0 (the authors are willing to share it):

- Get an estimation of the molar mass of the lubricant. No experimental data allowing to get the molar mass are available, the rough estimation $M = 200$ g·mol^{-1} will therefore be used.
- The critical compression factor must be fixed as usually, no good estimation can be obtained from experimental data. The recommended value is $Z_c = 0.2563$.
- The critical temperature and density must be determined using a modified Rackett equation (Equation 6). Two experimental density points of the pure oil can be used for that, if the temperature difference between the two points is large enough, which is the case. Then, the critical pressure can be deduced using the critical compression factor.

$$\rho = \rho_c Z_c^{-(1-\frac{T}{T_c})^{\frac{2}{7}}} \tag{6}$$

- One of the previously used density measurements can be re-used in the PVT equation of state to get an estimation of the acentric factor ω.
- No experimental point allows to get the isobaric heat capacity. The density being known, it can be estimated using the Liley and Gambil correlation (see Jia et al. (2020)):

$$c_p = \frac{0.75529 + 0.0034T}{\sqrt{\rho(288.15K)/998.5}} \tag{7}$$

- The estimation of the viscosity requires 4 "pure" lubricant viscosity data points. The four parameters used by the residual entropy scaling relation are therefore determined ($n_{\eta,k}$).
- No thermal conductivity data has been collected, no fitting of the residual entropy scaling relation for the thermal conductivity can therefore be carried out.
- Finally, the interaction parameter (k_{ij}) used in the Van der Waals mixing rule for the PTV EoS can be determined using one or more mixture bubble point pressures of the lubricant and the refrigerant R1233zd(E). Only a few data has been used here but over a wide temperature range to get more accuracy as higher pressure will be obtained, which induces less measurement errors as will be explained later.

After this procedure has been followed, the parameters of the "pure" lubricant are determined and can be found in Table 2. With those parameters, the PVT equation of state could be used to estimate the densities at the same temperatures as the collected experimental data. The relative deviation of the fitting can be found in Figure 5 for the density and in Figure 6 for the viscosity, where a good fitting is observed (relative deviation less 2% for both the density and the viscosity).

As mentioned previously, the fitting of the binary interaction parameter only relies on the bubble point pressure data. By definition, this paramameter can also influence the density computed with the equation of state. Nevertheless, as can be understood in Figure 7, the sensitivity of the density is relatively small compared to the viscosity, moreover, the diagram justifies the value of the binary interaction parameter, minimizing the Root Mean Square of the relative error with the experimental data.

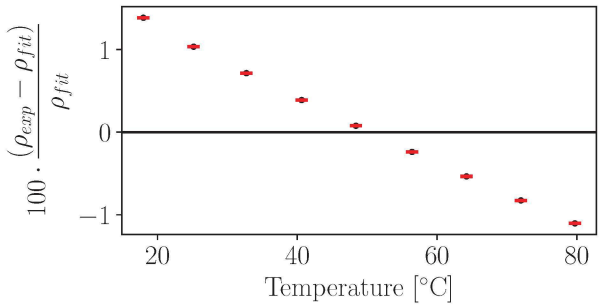

Figure 5: Relative error of experimental densities of POE RL32 from predictions of the model set with experimental uncertainties (red bars).

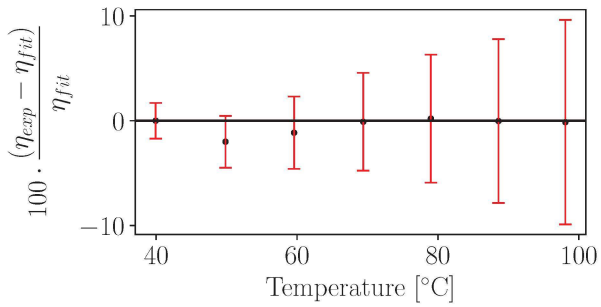

Figure 6: Relative error of experimental dynamic viscosities of POE RL32 from predictions of the model set with experimental uncertainties (red bars).

Table 2: "Pure" lubricant parameters estimated.

M [g/mol]	T_c [K]	ρ_c [kg/m^3]	Z_c [-]	P_c [bar]	ω [-]	k_{ij}	$n_{\eta,1}$	$n_{\eta,2}$	$n_{\eta,3}$	$n_{\eta,4}$
200	733.29	304.56	0.2563	23.8	0.8033	0.008	0.2649	-0.1055	0.0217	0.0000

4.2 Empirical correlations

The fitting of each empirical correlation has been done by minimizing the sum of the absolute errors between the predictions and the experimental data. The parameters of the five equations mentioned in Sections 3.1 and 3.2, have therefore been figured out. All the fitted parameters values can be found in Table 3. Furthermore, the empirical laws have been plotted in Figures 8, 9 and 10. These diagrams, in addition to show the good fitting between the experimental data and the correlations predictions, allow to see the whole experimental data set collected. Regarding the bubble point pressure data, the range comprises temperature from 10°C to 110°C with refrigerant liquid fraction from 15% to 95%. Regarding density and viscosity, less data could be obtained. On one hand, the range from 0% to 24.6% liquid refrigerant mass fraction could be covered by increasing the refrigerant mass little by little in the density-viscosity setup. On the other hand, the range from 100% to 94.2% liquid refrigerant mass fraction could be obtained by increasing the oil content. Unfortunately, no other valid data have been obtained with high refrigerant mass fraction due to a measurement problem.

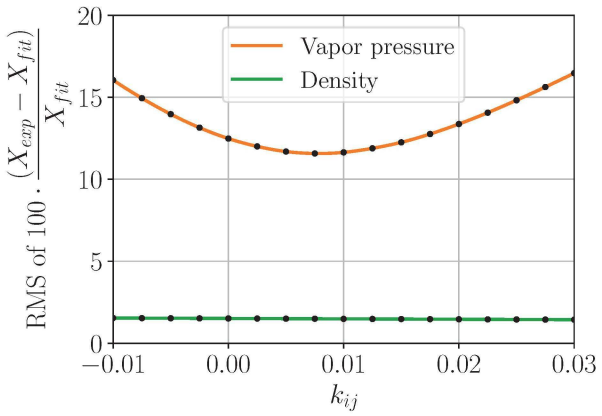

Figure 7: Sensitivity of the calculated density and bubble-point pressure with the binary interaction parameter k_{ij}.

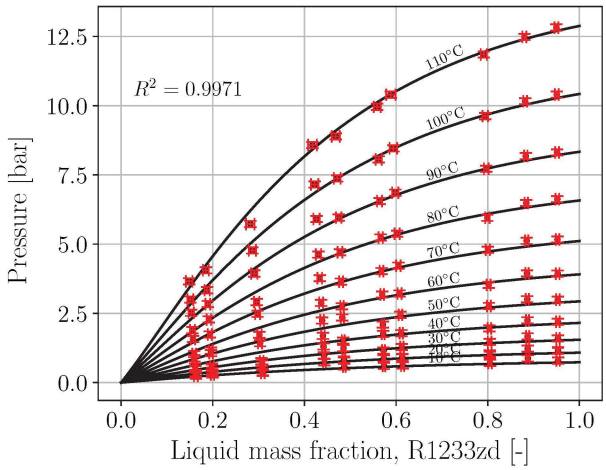

Figure 8: Vapor pressure predicted by Cavestri's equation and experimental data with uncertainties (red bars).

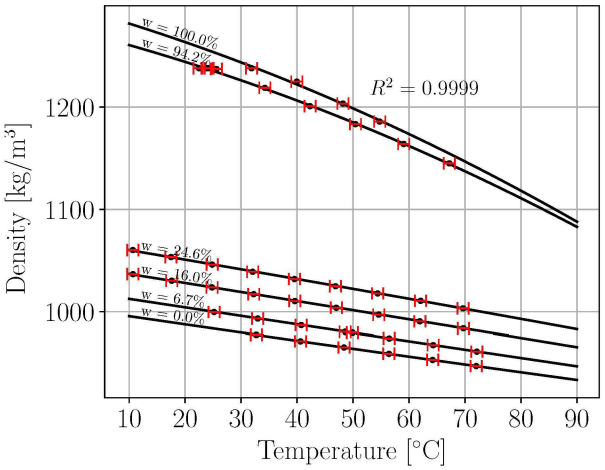

Figure 9: Mixture liquid phase density predicted by Henderson's equations and experimental data with uncertainties (red bars).

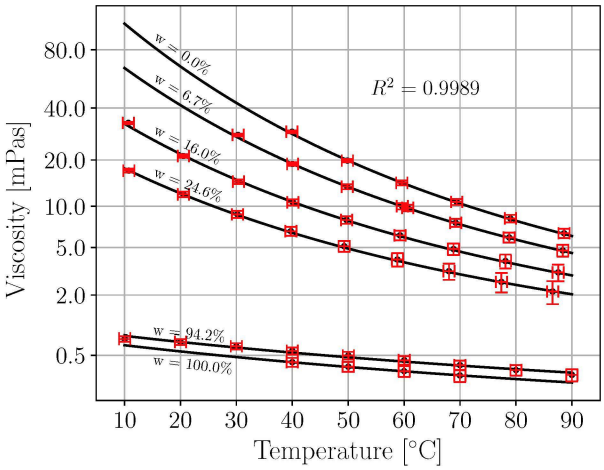

Figure 10: Mixture liquid phase dynamic viscosity predicted by Henderson's equations and experimental data with uncertainties (red bars).

Table 3: Empirical parameters of the Cavestri/Henderson equations.

	Cavestri Vapor pressure	Henderson - Density Low ref. fraction	Henderson - Density High ref. fraction	Henderson - Viscosity Low ref. fraction	Henderson - Viscosity High ref. fraction
a_1	$-4.81 \cdot 10^{-12}$	$1.2457 \cdot 10^{3}$	$-1.1405 \cdot 10^{3}$	$-2.5101 \cdot 10$	$-1.9406 \cdot 10^{-1}$
a_2	$-3.36 \cdot 10^{-9}$	$-9.6994 \cdot 10^{-1}$	$5.7927 \cdot 10^{3}$	$2.3716 \cdot 10$	$1.9977 \cdot 10^{2}$
a_3	$-2.04 \cdot 10^{-6}$	$3.0664 \cdot 10^{-4}$	$2.8966 \cdot 10^{3}$	-5.4460	1.2452
a_4	$4.18 \cdot 10^{-11}$	$1.7298 \cdot 10^{2}$	$3.7597 \cdot 10^{2}$	-4.1447	$-2.8316 \cdot 10^{-1}$
a_5	$1.42 \cdot 10^{-8}$	$9.6295 \cdot 10^{-1}$	$3.0111 \cdot 10^{2}$	4.7527	$1.8901 \cdot 10^{2}$
a_6	$4.74 \cdot 10^{-6}$	$-2.4620 \cdot 10^{-3}$	$-6.3891 \cdot 10^{2}$	-1.3613	1.1793
a_7	/	$3.1296 \cdot 10^{1}$	$1.8261 \cdot 10^{3}$	$2.7939 \cdot 10^{-1}$	-1.7167
a_8	/	$6.3640 \cdot 10^{-1}$	$-4.9566 \cdot 10^{3}$	2.2032	$1.7887 \cdot 10^{2}$
a_9	/	$-1.9274 \cdot 10^{-3}$	$-4.0906 \cdot 10^{3}$	-1.0525	1.1151

4.3 Comparison between the two models

In this section, the accuracy of both models is going to be compared. Graphs of relative errors and R^2 fitting indicators resulting from the thermodynamic approach of Yang et al. (2023a) and from the empirical correlations will be used to compare both modeling techniques. Moreover, experimental uncertainties will be added to the relative error calculations in order to check if these deviations can be explained by sensors inaccuracy or by the models themselves.

Firstly, the vapor pressure relative deviations of both models can be found in Figures 11 and 12 and, as can be observed, the graphs are very similar and the same goes for the R^2 indicators. An increase of the relative error is noticeable for low temperatures (i.e., < 50°C), where the pressures are low (< 2.5 bar according to Figure 8), moreover, the uncertainty also increases for low temperatures due to this low pressures as the absolute uncertainty of the pressure sensors is getting closer to the measured values. Therefore, the high relative errors of both models predictions could probably come from inaccurate measurements of the bubble point pressures.

Secondly, as can be seen in Figures 13 and 14, the density predictions of the thermodynamic model are good, with less than 3.5% of relative deviation, while the empirical model predicts the densities with an almost perfect fitting (R^2 = 0.9999). The measurement uncertainties do not influence the relative deviations in this case. Although a noticeable difference in accuracy can be observed between both models, it is important to keep in mind that the density prediction of the thermodynamic model only relies on a few "pure " lubricant fitted semi-empirical parameters, while the empirical correlations of Henderson, rely on 18 purely empirical parameters to be fitted in total (9 parameters for both low and high refrigerant concentrations).

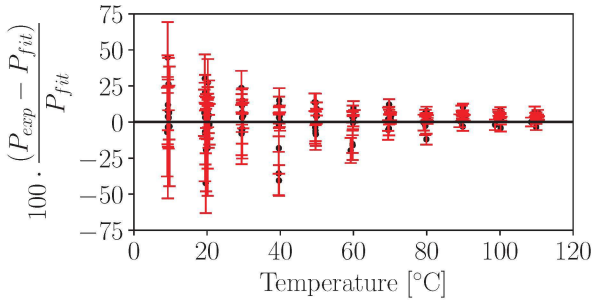

Figure 11: Relative error of the vapor pressure prediction from the PTV equation of state with experimental uncertainties (red bars) (R^2 = 0.9944).

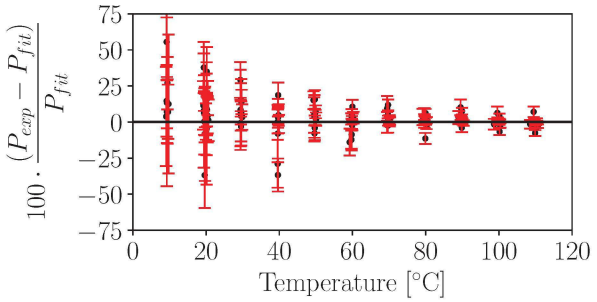

Figure 12: Relative error of the vapor pressure prediction from the Cavestri equation with experimental uncertainties (red bars) (R^2 = 0.9971).

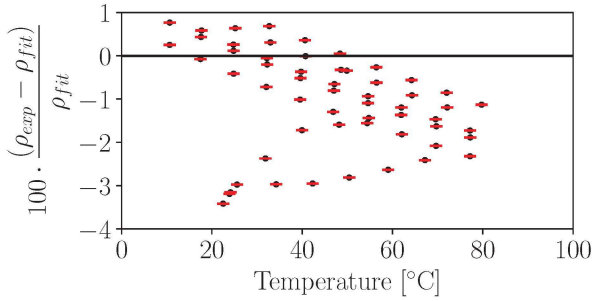

Figure 13: Relative error of the density prediction from the PTV equation of state with experimental uncertainties (red bars) (R^2 = 0.9617).

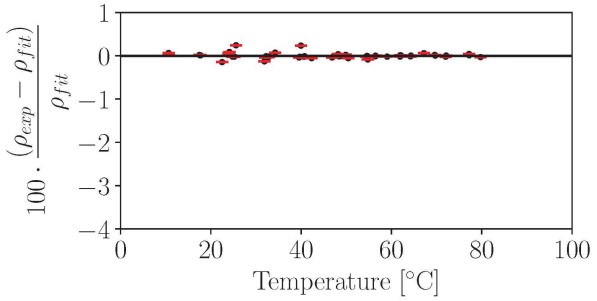

Figure 14: Relative error of the density prediction from the Cavestri equation with experimental uncertainties (red bars) (R^2 = 0.9999).

Finally, the relative deviations of the viscosity can be found in Figures 15 and 16. As can be observed, the predictions of the thermodynamic model are very bad (more than 50% of relative deviation), while those of the Henderson empirical equations are good (less than 5%). High measurement uncertainties are faced for the viscosity, however, seeing the low relative deviations of the empirical correlation and the uncertainty ranges, that are far from the zero line for the thermodynamic model, the uncertainty is certainly not the cause of those high relative deviations. Moreover, as stated in Yang et al. (2023a), viscosity prediction does not work well for strongly asymmetric mixtures, i.e., when the molecule sizes of the two "pure " components are very different, which is usually the case for oil-refrigerant mixtures.

In general, the comparison between both models clearly shows better performance of the empirical modeling techniques, in terms of accuracy. However, it is important to highlight other aspects of the modeling techniques, as in some cases, the accuracy is not always what matters the most. Firstly, in this specific scenario, lots of experimental data was collected, which allowed a very precise calibration of the empirical equations employed. With less data, such good calibration would not have been possible, whereas the fitting of the thermodynamic model would have been similar, as it mainly relies on pure fluids properties and can provide good fitting with a low number of experimental data. Secondly, except for the viscosity, the prediction of the thermodynamic model remains accurate. The accuracy is relative to what the predictions are needed for. Obtaining perfect predictions of thermodynamic properties is sometimes unnecessary when it is combined with other sources of uncertainties that propagates in the final results obtained. The most important and final argument towards thermodynamic modeling techniques is the sense of the physics behind those models. In particular, the parameters fitted for the "pure" lubricant have a physical sense. For instance, the critical point coordinates do have a meaning, even though it is not possible to measure them due to oil degradation with the too high temperatures involved. The thermodynamic model moreover allows to predict many different properties with one single model using correlated mechanism, such as the residual entropy scaling technique for the viscosity and the thermal conductivity.

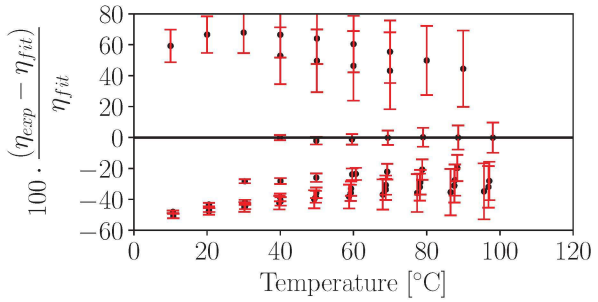

Figure 15: Relative error of the dynamic viscosity prediction from the RES with experimental uncertainties (red bars) (R^2 = 0.1910).

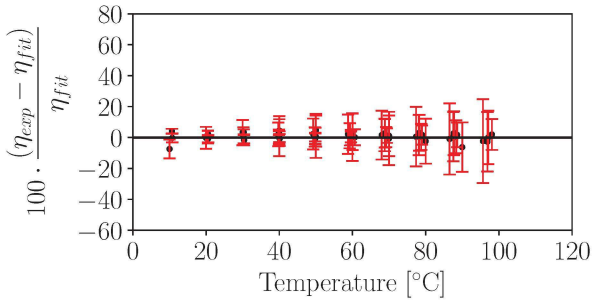

Figure 16: Relative error of the dynamic viscosity prediction from the Cavestri equation with experimental uncertainties (red bars) (R^2 = 0.9989).

5. CONCLUSION

In this work, the measurement results of the thermophysical properties of the lubricant POE Emkarate Rl32 MAF and its mixture with the refrigerant R1233zd(E) are presented with the focus on the bubble point pressure, the density and the dynamic viscosity. In particular, the investigation performed looks at the vapor pressure (bubble point), the density and the dynamic viscosity. Firstly, the setups used to collect the experimental data have been presented. The measurement uncertainty of both setups have been provided. Secondly, diverse modeling techniques allowing to predict properties of such mixture have been mentioned, and two of them have been calibrated with the experimental data investigated in terms of accuracy. The first modeling technique is the thermodynamic approach proposed by Yang et al. (2023a), where a low number of experimental data is required to calibrate the Patel-Teja-Valderrama cubic equation of state and residual entropy scaling approaches. The second modeling technique uses empirical correlations from Cavestri for the vapor pressure and from Henderson for the density and the viscosity to predict the mixture properties. The results show a better agreement with the experimental data for the empirical modeling approach for both the density and viscosity, while the vapor pressure data prediction accuracies are even in both approaches. In particular, the viscosity predictions of the thermodynamic approach are not good for the mixture with a root mean square relative error of 40%, which was expected knowing the strong asymmetry of the mixture used. Other aspects than the accuracy are also discussed, for instance the fact that empirical modeling requires a lot of experimental data to be calibrated while the thermodynamic approach requires only a low number of experimental data of the pure substances, which could sometimes be directly obtained from the manufacturer. Moreover, the physical meaning of the thermodynamic model and its versatility in terms of thermophysical property prediction make it a convenient option in many cases.

NOMENCLATURE

POE	Polyolester
PVT	Patel-Teja-valderrama
EoS	Equation of state
LV	Liquid-Vapor
P	Pressure
T	Temperature
c	Speed of sound
M	Molar mass
n	Empirical parameter
a_k	Empirical parameter
Z	Compressibility factor
x	Molar fraction
w	Mass fraction
k_{ij}	Binary interaction parameter
c_p	Isobaric heat capacity
n_μ	Residual entropy scaling parameter
Greek Symbols	(-)
η	Dynamic viscosity
ρ	Density
ω	Acentric factor
Subscripts and superscripts	
c	critical
r	reduced
ref	refrigerant
σ	saturation

REFERENCES

Bell, I. H. (2011). Theoretical and experimental analysis of liquid flooded compression in scroll compressors.

Briola, S., Gabbrielli, R., Baccioli, A., Fino, A., and Bischi, A. (2021). Thermo-economic analysis of a novel trigeneration cycle enabled by two-phase machines. *Energy*, 227.

Cavestri, R. C. (1995). Measurement of viscosity, density, and gas solubility of refrigerant blends in selected synthetic lubricants.

Dawo, F., Fleischmann, J., Kaufmann, F., Schifflechner, C., Eyerer, S., Wieland, C., and Spliethoff, H. (2021). R1224yd(z), r1233zd(e) and r1336mzz(z) as replacements for r245fa: Experimental performance, interaction with lubricants and environmental impact. *Applied Energy*, 288.

Henderson, D. R. (1994). Solubility, viscosity and density of refrigerant/lubricant mixtures.

Jia, X., Wang, J., Wang, X., Hu, Y., and Sun, Y. (2020). Phase equilibrium of r1234yf and r1234ze(e) with poe lubricant and thermodynamic performance on the evaporator. *Fluid Phase Equilibria*, 514.

Leclercq, N., Bederna, B. G., and Lemort, V. (2024). *Experimental Testing of a Scroll Compressor with Two-Phase Refrigerant Flows*, pages 239–250.

Neto, M. A. M. and Barbosa, J. R. (2011). Modeling the thermodynamic properties of refrigerant-oil mixtures and the effect of the oil circulation ratio on the performance of vapor compression systems.

Patel, N. C. and Teja, A. S. (1982). A new cubic equation of state for fluids and fluid mixtures. *Chemical Engineering Science*, 37:463–473.

Ramaraj, S., Yang, B., Braun, J. E., Groll, E. A., and Horton, W. T. (2014). Experimental analysis of oil flooded r410a scroll compressor. *International Journal of Refrigeration*, 46:185–195.

Scialdone, J. J., Miller, M. K., and Montoya, A. F. (1996). Methods of measuring vapor pressures of lubricants with their additives using tga and/or microbalances.

Stöckel, K., Nosbers, R., Barta, R. B., and Thomas, C. (2023). Measurement of vapour pressure, miscibility and thermal conductivity for binary and ternary refrigerant lubricant mixtures in the context of heat pump tumble dryers. *International Journal of Refrigeration*, 152:223–233.

Valderrama, J. O. (1990). A generalized patel-teja equation of state for polar and nonpolar fluids and their mixtures. *JOURNAL OF CHEMICAL ENGINEERING OF JAPAN*, 23:87–91.

Yang, X., Hanzelmann, C., Feja, S., Trusler, J. P., and Richter, M. (2023a). Thermophysical property modeling of lubricant oils and their mixtures with refrigerants using a minimal set of experimental data. *Industrial and Engineering Chemistry Research*, 62:18736–18749.

Yang, X., Xiao, X., Thol, M., Richter, M., and Bell, I. H. (2022). Linking viscosity to equations of state using residual entropy scaling theory. *International Journal of Thermophysics*, 43.

Yang, X., Xiong, X., Thol, M., Richter, M., and Bell, I. H. (2023b). A residual entropy scaling approach for viscosity of refrigerants, other fluids and their mixtures. 26th International Congress of Refrigeration (ICR).

Youbi-Idrissi, M. and Bonjour, J. (2008). The effect of oil in refrigeration: Current research issues and critical review of thermodynamic aspects.

ACKNOWLEDGMENT

The project source of the results presented in this paper has received funding from the European Union's Horizon 2020 research and innovation programme under grant agreement N° 851541.

I would like to acknowledge Benedikt Bederna from the TU Dresden for enabling the collection of the experimental data used in this study.